Optimization conversion of chitosan from Ganoderma lucidum spore powder using ultrasound-assisted deacetylation

Optimization conversion of chitosan from *Ganoderma lucidum* spore powder using ultrasound-assisted deacetylation: influence of processing parameters

Li-Fang Zhu[a,b], Xing Chen[b*], Zijing Wu[c], Guangkun Wang[c], Zeeshan Ahmad[d], Ming-Wei Chang [a,b,e *]

[a] Department of Biomedical Engineering, Key Laboratory of Ministry of Education, Zhejiang University, Hangzhou 310027, P.R. China.

[b] Zhejiang Provincial Key Laboratory of Cardio-Cerebral Vascular Detection Technology and Medicinal Effectiveness Appraisal, Zhejiang University, Hangzhou 310027, P.R. China.

[c]Tianhe Agricultural Group, Longquan, Zhejiang, 323700, P.R. China.

[d] Leicester School of Pharmacy, De Montfort University, The Gateway, Leicester, LE1 9BH, UK.

[e] Nanotechnology and Integrated Bioengineering Centre, University of Ulster, Jordanstown Campus, Newtownabbey, BT37 0QB, Northern Ireland, UK.

[*] Corresponding author: Ming-Wei Chang, Ph.D., Assoc. Professor

Tel: +86(0)571-87951517, Email: mwchang@zju.edu.cn; m.chang@ulster.ac.uk

Running Head: ultrasound-assisted conversion of chitosan

Abstract: Chitosan is an extremely valuable polysaccharide and usually obtained from crustacean byproduct. In this work, a new non-animal source chitosan is obtained from fungal precursors (*Ganoderma lucidum* spore powders, GLSP) using ultrasound-assisted deacetylation (USAD), and the effects of processing parameters (irradiation time, solid-to-liquid ratio, NaOH concentration, and irradiation power) on the DD (degree of deacetylation) of chitosan were investigated. The highest DD value was obtained at irradiation parameters of: 20 min, 10% (g: mL) NaOH, 1:25 (g: mL) and 80 W. In addition, the difference in surface morphology, chemical groups, thermal stability and crystallinity of the resulting chitosan with the treatment of various irradiation times were examined using the SEM, FTIR, TG and XRD. The results show a new promising herbal source of edible chitosan, and the potential material for biomedical applications.

Key words: chitosan; ultrasonics; deacetylation; optimization parameters; functional food.

Practical applications

The chitosan obtained from *Ganoderma lucidum* spore powders (GLSP) possessed many priorities over the chitosan from shells of crustaceans, which involves a multi-faceted procedure with several economical and consumer related aspects. In the current work, chitosan is obtained from an herbal source GLSP using ultrasound treatment and the effect of processing parameters on chitosan was investigated. The findings show

the development of chitosan from an herbal source with potential in functional food applications.

1. Introduction

Chitin, a white polysaccharide, not only in the exoskeleton of some insects and shellfish (e.g. crabs, shrimps, et al (Mohammed et al., 2013)), but also in the cellular wall of fungi and yeast (Álvarez et al., 2014). According to the molecular chain of N-acetyl-D-glucosamine joined by β- (1-4) glycosidic linkage (Fiamingo et al., 2016), there are three different polymeric forms of chitin: α, β and γ (Wan and Tai, 2013). Despite being the most abundant polymer after cellulose (Wan and Tai, 2013), chitin cannot be used raw unless it has been processed into nanofibers (Safari and Javadian, 2015) or converted into chitosan (Delezuk et al., 2011). Therefore, the modifications of chitin using chemical methods (Sagheer et al., 2009) or ultrasound irradiation (Birolli et al., 2016) have been established to make full use of chitin. Chitosan, one of the most amount polycationic polysaccharides (Menezes Maciel Bindes et al., 2019), which is obtained from chitin following deacetylation (Roberts, 1992). Some authors considered the derivative could be named chitosan when the degree of deacetylation (DD) was higher than 60% only (Anitha et al., 2014), or whilst others have stated 50% was also enough (Sagheer et al., 2009).

During the deacetylation process, the GlcNAc unit which is present in chitin converts to GlcN and this this the unit that exists in chitosan (Fiamingo et al., 2016). Due to its biocompatibility, non-toxicity and biodegradability (Delezuk et al., 2011), chitosan has showed various applications in the biomedical engineering field including but not limited to drug delivery (Dev et al., 2010), wound healing (Radhakumary et al., 2011) and tissue engineering (Ragetly et al., 2010).

As a result of increased demands for chitosan, deacetylation methods and sources of chitin have diversified (Pariser and Lombardi, 1989). Traditionally, thermochemical deacetylation (TCD) has been used to convert chitin to chitosan. TCD involves treatment using concentrated (30-50%) sodium hydroxide or potassium hydroxide solutions combined with relatively high temperatures (80-115°C) and prolonged processing time (1-6 hours) (Kurita, 2001; Lamarque et al., 2004). The reactions that occur during processing are heterogenous which leads to variation of key characteristics and properties of the yielded chitosan (Khong et al., 2012). In addition to this, due to the harsh conditions required to yield chitosan, depolymerization cannot be avoided (Lamarque et al., 2007). Therefore, many new methods have been proposed to overcome the these limitations including microwave-assisted deacetylation (Dahmoune et al., 2015), ultrasound-assisted deacetylation (USAD) (Fiamingo et al., 2016) and enzyme-assisted process (Tokuyasu et al., 2000).

USAD has proved to be an efficient process to convert chitin into chitosan. High temperatures (5000-10000K) and high pressures (~100 MPa) can be controlled by using cavitation effects of ultrasound irradiation in localized treatment (Godínez et al., 2012).

Therefore, deacetylation can be achieved at lower temperatures (50-80°C) with shorter reaction times (10-60 min), both of which have contributed to the reduction of depolymerization risk (Price, 2003).

The work presented here sourced chitosan from *Ganoderma lucidum* spore powder (GLSP) using the single probe USAD process. The effects of the process parameters on the characteristics of the obtained chitosan was discussed and the said parameters were optimized using the Taguchi orthogonal array design. The surface morphology, thermostability and the solid state of the resulting chitosan was determined using SEM, TG and X-ray diffraction, respectively. The results reported in this study may offer a new alternative source of chitosan, and improve the additional value of GLSP relics.

2. Materials and Methods

2.1 Materials

GLSP (TianHe Agricultural Group, ZheJiang Long Quan, China) was converted to GLSP relics after being extracted according to previous work (Yao et al., 2017) and were dried using a vacuum oven (D2F-6020AF, Tianjin GongXing Laboratory Instrument Co., Ltd., Tianjin, China) at 65 °C, ~0.95MPa for 3 days. Hydrogen peroxide 30% (H_2O_2 solution), hydrochloric acid, sodium hydroxide (troche), sodium chloride (pulvis) and acetic acid were chemical pure and obtained from Sinopharm Chemical Reagent Co., Ltd. (Shanghai, China). DI water (deionized water) was produced by the Millipore Milli-Q Reference ultrapure water purifier (Millipore, Bedford, USA). Commercial chitosan ($C_{6n}H_{11n}NO_{4n}$) was purchased from Macklin

(Macklin Biochemical Co., Ltd., Shanghai, China). All chemicals did not have further purification prior to experimentation.

2.2 Preparation of chitosan using USAD process

The dried GLSP relics were bleached using H_2O_2 solution at 70 ℃ for 2 h until they were light yellow in appearance. The relics were then neutralized using NaOH solution and the sediment was collected via centrifugation at 22°C at 10,000 rpm for 10 mins (Centrifuge 5810 R, Eppendorf, Germany). For the USAD process, the sediment was suspended in a 10% w/v NaOH solution at the ratio of 1:25 (g: mL) in wide mouth bottles and were subjected to ultrasound irradiation using a horn-type transducer (Φ =13 mm, 20 kHz, 200 W, Sonifier 250m Branson Ultrasonics Co., Ltd). A schematic diagram is shown in Figure 1a. During the entire experiment the water in the tank was kept at constant volume (2.5 L) and the same distance between the bottles and transducers were also kept constant at 20 mm. following irradiation, the sediment was collected via centrifugation just as in section **2.1**. In this study, the sonication setup was equipped with a custom-made refreshing bath allowing the temperature of GLS suspension to be monitored and controlled to a temperature of 36.1 °C. It was found that the temperature of the transducer and the GLS suspension increased with irradiation time (Figure 1b), implying the deionized water will increase to 36.1°C when irradiation duration was 30 minutes. Therefore, the experiments here was limited below 30 mins in order to minimize the effect of temperature.

2.3 Characterization

2.3.1 Morphology assessment

The effect of ultrasound irradiation on the morphology of the resulting chitosan was analyzed using field emission scanning electron microscopy (FESEM) (SEM, Quanta FEG650, FEI, China). Samples were coated with a thin layer of gold using a sputter-coater (108 Auto Cressington Sputter Coater, Ted Pella, INC.) under vacuum for 60 s with 25 mA current intensity.

2.3.2 DD (degree of deacetylation), [η] (dynamic viscosity) and $\overline{Mv}$ (viscosity average molecular weight) measurements

The degree of deacetylation (DD) was calculated using Eq. (1) and (2) (Brugnerotto et al., 2001).

$$A_{1320}/A_{1420}=0.3822+0.03133DA \quad (1)$$

$$DD\ (\%) = 1-DA \quad (2)$$

Where, A_{1320} and A_{1420} was the absorbance value obtained from FTIR at 1320 cm^{-1} and 1420 cm^{-1}, respectively. DA was the acetylation degree.

The [η] was measured using a viscometer (DV2TLVCJ0, Brookfield, USA) at ambient temperature (25 ℃). In brief, a number of resulting chitosan 0.2 M NaCl and 0.1 M acetic acid solution was prepared with a ratio of 1:1 (v: v) in advance, then adding to get suspension. Before measuring the viscosity, the suspension was treated using an ultrasonic device (40 kHz, KS-300 EI, Kesheng, Co., Ltd, Zhejiang, China) for 30 mins

at ambient temperature (25°C) to obtain a homogenous solution. The [η] was calculated with Eq. (3)– (5) (Shangan Lin, 1998).

$$\eta_{sp} = \frac{\eta - \eta_0}{\eta_0} \quad (3)$$

$$\eta_r = \frac{\eta}{\eta_0} \quad (4)$$

$$[\eta] = \frac{1}{c}\sqrt{2(\eta_{sp} - \ln\eta_r)} \quad (5)$$

Where, the η_0 and η was the solution and suspension viscosity, respectively. And η_{sp} is the value viscosity of specific viscosity, the η_r is relative viscosity, c is the concentration of chitosan in the suspension, g/ mL.

The $\overline{\mathrm{Mv}}$ was calculated with Mark–Houwink–Sakurada Eq. (6) (Kasaai et al., 2015):

$$[\eta]=\kappa\,\overline{\mathrm{M}}\mathrm{v}^{\alpha} \quad (6)$$

where, the variable parameters $\kappa=1.81\times10^{-3}$ L/ g and $\alpha=0.93$ (Maghami and Roberts, 2010), which depended on solution and temperature (Wang et al., 1991).

The orthogonal array design $L_9(3^4)$ (Table 1) was employed to optimize the irradiation parameters.

2.3.3 Fourier transform infrared spectroscopy (FT-IR) assay

The effect of ultrasound irradiation on the presence or absence of functional groups in the yielded chitosan was confirmed using FT-IR spectroscopy (IR Affinity 1, Shimadzu, Japan). Sample pellets were prepared by mixing the sample with KBr powder according to the method stated in previous work (Zhi-Cheng Yao, 2016). FTIR spectrums were obtained by scanning a range from 4000-400cm^{-1} at a resolution of 4 cm^{-1}.

2.3.4 X-Ray Diffraction (XRD)

XRD assay on the resulting chitosan was carried out using a X-ray diffractometer (Gemini A OHra, Oxford Varian, UK) with the following parameters: 1˚of DivSlit, 10 mm of DivH.L.Slit, diffraction range (2θ) of 3-60˚, and examined at 40 kV/30 mA. Scanning deploying step and step speed was 0.02˚ and 5˚/min, respectively. Thus, the crystalline index (CrI) was calculated using the Eq. (7) (Sayari et al., 2016):

$$CrI_{110}(\%) = [(I_{110}-I_{am})/I_{110}] \times 100 \qquad (7)$$

where, I_{110} and I_{am} was the maximum diffraction intensity and amorphous diffraction intensity at 2θ≈ 20˚ and 13˚, respectively.

2.3.5 Thermogravimetric analysis (TGA)

Thermal behavior of the resulting chitosan was revealed via TGA analysis. A thermogravimetric analyser (TGA/DSC1 device, Mettler-Toledo, UK). The samples were heated at a rate of 10 °C min^{-1} from 31°C to 700°C under atmospheric conditions.

2.4 Statistical analysis

Data for all experiments were performed in triplicate and were given as mean ± standard deviation (n=3). Statistical analysis was performed using SPSS ((Statistic Package for Social Science)) software (SPSS Statistics v20.0, IBM, UK). An $L_9(3^4)$ Taguchi design of experiment was used to evaluate the effects of four factors (Time, NaOH concentration, Solid-liquid ratio, and irradiation Power) on the resulting chitosan

physicochemical properties (DD, [η] and $\overline{Mv}$). ANOVA was used to compare the results between multiple groups and to optimize the treatment parameters. The F-value is a statistic of F-test, SS-value is the sum of squares, and p-value the is significance of one factor on the results. The significant order priority of the effect of four factors on the result was determined according to the order from large to small of F-value. The p-value was labeled with * if the p-value was smaller than 0.05 calculating by SPSS. Then, the optimal level for the each of four parameters can be selected based on the range analysis (Kij values). These three results (F-value, SS-value, and p-value) were obtained from SPSS software. All statistical plots were plotted using Origin software (Origin Lab, USA).

3. Results and discussion

3.1 Effect of USAD on the DD, [η], $\overline{Mv}$, and yield

Sonication is an emerging technology that was initially developed to minimize processing, maximize quality and ensure safe delivery of bio-products. In order to optimize the USAD process for herbal based chitosan preparation, the application of ultrasound under various process parameters (irradiation time, concentration of NaOH, solid-liquid ratio, duty cycle (on time: off time, min: min) and power) on [η], $\overline{Mv}$ and DD was investigated (Figure 2).

Figure 2a shows the effect of irradiation time on DD, [η] and $\overline{Mv}$. The power (50 W), concentration of NaOH (10%, g: mL), solid-liquid ratio (1:10, g: mL) and duty cycle (no off time) were kept constant. The DD value increased with increasing irradiation

time, and the maximum DD value (79.9 %) was obtained at the 30 min irradiation time. The [η] and $\overline{Mv}$ was decreased as the prolonged time. This phenomenon was attributed to the cavitation effect: high temperature and pressure which had accumulated. Hence, more GlcNAc (2-acetamido-2-deoxy-D-glucopyranose) units in chitin were converted to GlcN (2-amino-2-deoxy-D-glucopyranose) units during the extended USAD process. and chain scission and depolymerization induced by ultrasound (Delezuk et al., 2011; Simina et al., 2009), so the [η] and $\overline{Mv}$ decreased.

Figure 2b shows the effect of power on DD, [η] and $\overline{Mv}$. The time (10 min), concentration of NaOH (10%, g: mL), solid-liquid ratio (1:10, g: mL) and duty cycle (no off time) were kept constant. When the irradiation power increased from 20 W to 160 W, the DD increased from 75.4% to 83.1%. [η] decreased from 148.1 cP to 59.1 cP, and $\overline{Mv}$ decreased from 1.9×10^5 g/mol to 7.1×10^4 g/mol was irradiation power was increased. It confirmed that higher ultrasound irradiation power can be used to prepare chitosan with higher DD value, lower [η] and $\overline{Mv}$ value. This may be attributed to the fact that the conversion of deacetylation of chitin into chitosan is a heterogeneous process, which is dependent on the accessibility of reaction agent (alkaline group) to the reactive site (Delezuk et al., 2011). In addition to this, higher ultrasound power can generate higher energy and stronger cavitation activity, improving the accessibility to the reactive sites and enhancing the depolymerization rate (Delezuk et al., 2011). Therefore, greater irradiation power reduces the acetyl content and yields shorter molecular chains of chitosan; inducing the resulting chitosan with lower [η] and lower $\overline{Mv}$ value.

Figure 2c shows the effects of NaOH solution concentration on [η], $\overline{Mv}$ and DD. For this irradiation time (10 min), power (50 W), solid-liquid ratio (1:15, g: mL), duty cycle (no off time) were kept constant. The DD value increased with increasing NaOH concentration; increasing from 67.2% to 83.2% when the NaOH concentration was increased from 5% to 40%. [η] and $\overline{Mv}$ decrease as the NaOH concentration increasing, from 174.1 cP to 47.1 cP and 2.3×10^5g/mol to 5.6×10^4g/mol, respectively. This may be due to the fact that the higher concentration of alkaline solution can promote more GlcNAc units of chitin by converting the GlcN unit of chitosan, thus inducing the depolymerization process via oxidative alkaline hydrolysis (Delezuk et al., 2011).

Figure 2d shows the effect of solid-liquid ratio on [η], $\overline{Mv}$ and DD. For this, the irradiation time (10 min), NaOH (20%, g: mL), power (80 W), duty cycle (no off time) were kept constant. When the solid-liquid ratio is increased from 1:5 to 1:25 (g: mL), the DD increases slightly from 81.0% to 82.5%. [η] and $\overline{Mv}$ increased with increasing solid-liquid ratio from 1:5 to 1:15 (g: mL), but the reverse trend is noted when the solid-liquid ratio is more than 1:15 (g: mL). The maximum values of [η] and $\overline{Mv}$ were 110.1 cP and 1.4×10^5g/mol, respectively, when the solid-liquid ratio is 1:15 (g: mL). It was observed that increasing the solid-liquid ratio to more than 1:15 decreased the values of [η] and $\overline{Mv}$. This may be attributed to the fact that a solid-liquid ratio more than 1:15 means there was more liquid (NaOH solution) than solid (GLSP relics). Subsequently, the depolymerization process was improved since using dilute solvent can minimize the depolymerization (Sannan et al., 1975).

Figure 2e shows the effect of duty cycle on DD, [η] and $\overline{Mv}$. For this the irradiation time (30 min), NaOH (10%, g: mL), solid-liquid ratio (1:15, g: mL), power (80 W) were kept constant. During this experiment, the length of each off time was 1 min and the number of off time was variable. Prolonging the off time leaded to an increase in both [η] and $\overline{Mv}$, which most likely resulted from the cavitation effect of ultrasound which weakened for the length of each irradiation process was shorten as the increase of the number of off time, then the depolymerization was weaken and so the [η] and $\overline{Mv}$ increased. The maximum value of DD was obtained at duty cycle of 30: 1, in which the off time was 1 min and the irradiation time (30 min) was divided into two parts. The DD results indicated much or less than the suitable off time will hinder the deacetylation process, which may be attributed to the fact that the contact of reactive site with sodium hydroxide solution was affected by the length of continuous irradiation each time and the frequency of off time set.

It can be concluded that DD is affected by the irradiation power, irradiation time, NaOH concentration, solid-liquid ratio and duty cycle. Therefore, USAD is able to carry out chitosan conversion by deacetylating the GlcNAc unit with high DD, [η] and $\overline{Mv}$. while, the severe depolymerization should be given to avoid, since the continuous irradiation will induce chain scission and depolymerization (Simina et al., 2009).

Figure 2f shows the effects of irradiation time on the yield of chitosan (%yield = $m_c/m_G \times 100\%$, m_c: mass of chitosan, g; m_G: mass of GLSP, g). For this, the irradiation power (120 W), NaOH (20%, g: mL), solid-liquid ratio (1:15, g: mL), duty cycle (no off time) were kept constant. It was observed that the yield increased from 68.7% to

89.9% as the irradiation time was increased from 5 mins to 30. This may be attributed to the fact that a longer irradiation time allows more chitin to be converted to chitosan, and more soluble ingredients (such as polysaccharide) are removed, thus the yield of resulting chitosan increases. The increased yield of chitosan between 20 mins and 30 mins was smaller than that was observed between 5 and 10 mins; highlighting there was a plateau for irradiation time, which is consistent with the application of ultrasound-assisted extraction of targets (Xu et al., 2017).

3.2 Effect of USAD on the resulting chitosan morphology

The effect of USAD with various irradiation times on the chitosan was revealed from the differences in morphology (Figure 3). Chitosan yielded from USAD showed to have smooth surface (Figure 3b-e) when compared to the surface of the raw material (Figure 3a). The original oval and intact shape of the raw material is absent after USAD processing, with the oval shape only being vaguely visible in Figure 3b. the lack of the oval shape may be sue to the ultrasound treatment time being only 5 minutes, hence the cavitation effects did not have sufficient time to break the GLSP structure. The relatively smoother surfaces morphology showed in Figure 3c-e as compared with that of Figure 3b, result from prolonged irradiation time. Some shallow ridge-like bulges can be seen in Figure 3c with chitosan samples obtained from irradiation for 10 mins while the chitosan obtained from 20 or 30 mins of treatment (Figure 3d & e) exhibited much smoother surfaces. These results confirmed that the effect of ultrasound irradiation time on the resulting chitosan surface morphology was significant, and that

prolonged irradiation time can yield chitosan with much smoother surface morphology. The difference in surface morphology during the USAD process may be due to the oval structure being destroyed, leaving some shallow ravines the irradiation time was about 10 min. The surface morphology then became smoother when these ravines disappeared following further irradiation (ca. 20 min). Some microvillus formed when the irradiation time was 30 min. In conclusion, the cavitation effect generated from ultrasound irradiation can smooth the rugged surface, and then break the smooth surface again and the bulk mass will turn into the small particles when the treatment is sufficient enough.

3.3 FT-IR and XRD analysis

FT-IR spectroscopy is a useful tool to obtain the information about band properties and intensities, therefore, the variation in the number of entities resulted from chemical process can be identified (Osman and Arof, 2003). The FT-IR spectroscopy results revealed that there were no significant differences among the presence or absence of functional groups of the resulting chitosan samples, which showed the strong resemblance with the purchased chitosan. As the spectrum shows in Figure 4a, the absorbance peak of β-(1,4) glycosidic that exists in chitosan arose at 878 cm^{-1} (Kumari et al., 2015); the amid I, a characteristic band for chitosan, arose at 1656 cm^{-1} and 1621 cm^{-1} for α-chitosan and 1626 cm^{-1} for β-chitosan (Kucukgulmez et al., 2011). The absorbance peaks exhibited at 1320 cm^{-1} were characteristic of -NH_2, -OH, and -CO groups (Mahlous et al., 2007); and the absorbance peaks shown at 1420 cm^{-1} is

indicative of CH_2 deformation (Mauricio-Sánchez et al., 2018). The stretching vibration of -C-O-C reside in glucosamine ring and -CN of acetamide group arose at 1028 cm^{-1} and 1455 cm^{-1}, respectively; and the absorbance peak appeared at 2927 cm^{-1} was the vibration of $-CH_3$; other absorbance peaks for chitosan as follows: stretching C-H (2918 and 2878 cm^{-1}), stretching C=O (1647 cm^{-1}), bending NH_2 (1597 cm^{-1}) (Kumari et al., 2015). Also, the purchased chitosan showed an obvious absorbance peak at 1655 cm^{-1}, corresponding to band of amide I (Mauricio-Sánchez et al., 2018). The intensity of this peak decreased as irradiation time increased, highlighting that the deacetylation process reduced amide content. These results are consistent with a study carried out by Badawy et al (Badawy and Mohamed, 2015). The absorbance peak at 1655 cm^{-1} of raw material-GLSP FTIR spectra was more obvious than that of resulting chitosan, which confirmed the amide content in GLSP was higher than that of chitosan (Badawy and Mohamed, 2015). Moreover, the differences among the absorbance peak intensities may be as a result of the different time periods of irradiation, which generated a difference in cavitation effect.

XRD analysis was performed to characterize and verify any polymorphs of chitin, since the XRD pattern of chitosan was much broader and less intense peaks were observed after the deacetylation process, when comparing with chitin (Delezuk et al., 2011). As the XRD results show in Figure 4b and Table 2, in the work of Kaya et al., the characteristic peak appeared at $2\theta \approx 21.1^{\circ}$ (Kaya et al., 2015), while the peaks of resulting chitosan in this study appeared at $2\theta \approx 20.9^{\circ}$. Additionally, the four spectra showed new intense peaks which shifted to higher 2θ, which was consistent with the

previous works (Sagheer et al., 2009; Sayari et al., 2016). The emerging new intense peaks indicated the deacetylation process triggered new peaks shifting toward higher 2θ. Moreover, the characteristic XRD peaks of chitosan from mushroom also revealed similar diffraction peaks at around 20.30˚and 20.01˚, respectively (Erdogan et al., 2017).

3.4 TGA

The effect of USAD on the thermal stability of the resulting chitosan was investigated using TG analysis. It was found that the thermal stability of chitosan was less than that of chitin due to the acetyl content is lower in chitosan (Tang et al., 2005). The TGA results (Figure 5a) shows the chitosan yielded from various irradiation times exhibited similar behaviors in the range of 30-700 ℃. The degradation process was triphasic with the first stage occurring between 31 and 128 ℃ being the initial weight lost due to evaporation of water absorbed on the surface and bound to the chains' (Delezuk et al., 2011). The second weight loss event occurred at ~ 369°C due to the degradation of saccharide and deacetylated chitin units (Paulino et al., 2006). The largest weight loss event occurred between 370 and 477 ℃. This was due to polymer degradation (Álvarez et al., 2014). As highlighted in Table 3, the final residual weight proportion of chitosan from 5 mins irradiation time was higher than that of 10 min, and chitosan from 20 min treatment was higher than that of 30 min. The final residual weight proportion of chitosan from 5 min and 10 min was approximately equal to that of 20 min and 30 min, respectively. The final residual weight proportion change tendency of these chitosan samples was consistent with the results of CrI (Table 2). It confirmed that the thermal-stability of chitosan differed between chitosan with various CrI; with chitosan with the

highest CrI was more stable at the temperature interval of 478 – 700 ℃, and the hydrolysis of acetamido groups trigged by the alkaline solution (Mazeau et al., 1994) will result in more unordered chitosan chains when compared to chitin (Lavall et al., 2007).

Figure 5b shows temperature related degradation speed for these samples, which is a differential curve of Figure 5a. The minimum DTG value of the chitosan samples was obtained at the same temperature (ca. 416 ℃), and these minimum values change tendency were consistent with results of CrI (Table 2).

3.5 The optimization of USAD parameters

This study evaluated the effects of USAD parameters on DD, [η] and $\overline{Mv}$. Based on the results of single-factor experiments (section 3.1) and in view of the economic cost, four variables (time, NaOH concentration, solid-liquid ratio, power) were selected to identify the optimum parameters. The DD was selected as the dependent variable for the orthogonal test as it plays an important role in the properties of chitosan including solubility, biological activities, chemical and physical characteristics (Cho et al., 2000).

The Taguchi's orthogonal array results are shown in Table 4, which revealed the significance of main effects. The optimal irradiation parameters of USAD were acquired through range analysis. The DD ranged from 80.75% to 83.99% (Table 4). In USAD, the parameter contributions on DD were NaOH concentration＞solid-liquid ratio＞time＞power ($P < 0.001$). In addition, the optimal level for the each of four parameters can be revealed based on the range analysis (Kij values). The theoretical

maximum DD can be obtained at 10 min, 30% (g: mL) NaOH, 1:25 (g: mL) and 120 W.(Dev et al., 2010)

4. Conclusion

The work presented here demonstrated the efficiency of USAD to convert GLSP into chitosan using aqueous sodium hydroxide solution. By introducing USAD, the values of DD, [η] and $\overline{Mv}$ of obtained chitosan were varied depending on specific process parameters. Higher power, longer irradiation times and higher concentration of sodium hydroxide treatment yielded chitosan with higher DD value but lower values of [η] and $\overline{Mv}$. The optimal irradiation parameters of USAD were acquired through results of an orthogonal experiment, and the parameter contributions on DD were NaOH concentration > solid-liquid ratio > time > power ($P < 0.001$). The surface morphology, functional groups and thermal stability were varied as the different time irradiation treated. The thermal-stability of chitosan differed between chitosan with various CrI; with chitosan with the highest CrI was more stable at the temperature interval of 478 – 700 ℃. GLSP was effective as a new source of chitosan, and USAD was an excellent method to yield the chitosan.

Acknowledgements

This work was financially supported by the National Nature Science Foundation of China (No. 81301304), the Key Technologies R&D Program of Zhejiang Province (2015C02G2010104; 2015C02035) and the Research Fund for The Doctoral Program of Higher Education of China (20130101120170).

Competing interests

There are no conflicts to declare.

Corresponding Authors

* Email: m.chang@ulster.ac.uk

References

Álvarez, O.S.P., Ramírez Cadavid, D.A., Escobar Sierra, D.M., Ossa Orozco, C.P., Rojas Vahos, D.F., Zapata, O.P., Atehortúa, L. 2014. Comparison of extraction methods of chitin from Ganoderma lucidum mushroom obtained in submerged culture. Biomed. Res. Int. 2014**,** 169071.http://doi.org/10.1155/2014/169071

Anitha, A., Sowmya, S., Kumar, P.T.S., Deepthi, S., Chennazhi, K.P., Ehrlich, H., Tsurkan, M., Jayakumar, R. 2014. Chitin and chitosan in selected biomedical applications. Prog. in Polym. Sci. 39**,** 1644-1667.http://doi.org/10.1016/j.progpolymsci.2014.02.008

Badawy, R., Mohamed, H. 2015. Chitin extration, Composition of Different Six Insect Species and Their Comparable Characteristics with That of the Shrimp.http://www.jofamericanscience.org

Birolli, W.G., Delezuk, J.A.D.M., Campana-Filho, S.P. 2016. Ultrasound-assisted conversion of alpha-chitin into chitosan. Appl. Acoust. 103**,** 239-242.http://doi.org/10.1016/j.apacoust.2015.10.002

Brugnerotto, J., Lizardi, J., Goycoolea, F.M., Argüelles-Monal, W., Desbrières, J., Rinaudo, M. 2001. An infrared investigation in relation with chitin and chitosan characterization. Polymer. 42**,** 3569-3580.https://doi.org/10.1016/S0032-3861(00)00713-8

Cho, Y.W., Jang, J., Park, C.R., Ko, S.W. 2000. Preparation and solubility in acid and water of partially deacetylated chitins. Biomacromolecule. 1**,** 609-614.http://doi.org/10.1021/bm000036j

Dahmoune, F., Nayak, B., Moussi, K., Remini, H., Madani, K. 2015. Optimization of microwave-assisted extraction of polyphenols from Myrtus communis L. leaves. Food Chem. 166**,** 585-595.http://doi.org/10.1016/j.foodchem.2014.06.066

Delezuk, J.A.D.M., Cardoso, M.B., Domard, A., Campana-Filho, S.P. 2011. Ultrasound-assisted deacetylation of beta-chitin: influence of processing parameters. Polym Int. 60**,** 903–909.http://doi.org/10.1002/pi.3037

Dev, A., Binulal, N.S., Anitha, A., Nair, S.V., Furuike, T., Tamura, H., Jayakumar, R. 2010. Preparation of poly(lactic acid)/chitosan nanoparticles for anti-HIV drug delivery applications. Carbohyd. Polym. 80**,** 833-838.http://doi.org/10.1016/j.carbpol.2009.12.040

Erdogan, S., Kaya, M., Akata, I. 2017. Chitin extraction and chitosan production from cell wall of two mushroom species (Lactarius vellereus and Phyllophora ribis). AIP Conference Proceedings. 1809**,** 020012.https://doi.org/10.1063/1.4975427

Fiamingo, A., Delezuk, J.A., Trombotto, S., David, L., Campana-Filho, S.P. 2016. Extensively deacetylated high molecular weight chitosan from the multistep ultrasound-assisted deacetylation of beta-chitin. Ultrason Sonochem. 32**,** 79-85.http://doi.org/10.1016/j.ultsonch.2016.02.021

Godínez, F.A., Navarrete, M., Sánchez-Ake, C., Mejía-Uriarte, E.V., Villagrán-Muniz, M. 2012. Spectroscopic and thermodynamic features of conical bubble luminescence. Ultrason Sonochem. 19**,** 668-681.http://doi.org/10.1016/j.ultsonch.2011.08.011

Kasaai, M.R., Arul, J., Charlet, G. 2015. Intrinsic viscosity–molecular weight relationship for chitosan. J. Polym. Sci. Pol. Phys. 38**,** 2591-2598.http://doi.org/10.1002/1099-0488(20001001)38:19<2591::aid-polb110>3.0.co;2-6

Kaya, M., Baublys, V., Šatkauskienė, I., Akyuz, B., Bulut, E., Tubelytė, V. 2015. First chitin extraction from Plumatella repens (Bryozoa) with comparison to chitins of insect and fungal origin. Int J Biol Macromol. 79**,** 126.https://doi.org/10.1016/j.ijbiomac.2015.04.066

Khong, T.T., Aachmann, F.L., Vårum, K.M. 2012. Kinetics of de- N -acetylation of the chitin disaccharide in aqueous sodium hydroxide solution. Carbohyd. Res. 352**,** 82-

87.https://doi.org/10.1016/j.carres.2012.01.028

Kucukgulmez, A., Celik, M., Yanar, Y., Sen, D., Polat, H., Kadak, A.E. 2011. Physicochemical characterization of chitosan extracted from Metapenaeus stebbingi shells. Food Chem. 126**,** 1144-1148.http://doi.org/10.1016/j.foodchem.2010.11.148

Kumari, S., Rath, P., Kumar, A.S.H., Tiwari, T. 2015. Extraction and characterization of chitin and chitosan from fishery waste by chemical method. Environ. techno. Innov. 3**,** 77-85.http://doi.org/10.1016/j.eti.2015.01.002

Kurita, K. 2001. Controlled functionalization of the polysaccharide chitin. Prog Polym Sci. 26**,** 1921-1971.http://doi.org/10.1016/S0079-6700(01)00007-7

Lamarque, G., Chaussard, G., Domard, A. 2007. Thermodynamic aspects of the heterogeneous deacetylation of beta-chitin: reaction mechanisms. Biomacromolecule. 8**,** 1942.http://doi.org/10.1021/bm070021m

Lamarque, G., Christophe Viton, A., Domard, A. 2004. Comparative Study of the First Heterogeneous Deacetylation of α- and β-Chitins in a Multistep Process. Biomacromolecule. 5**,** 992-1001.http://doi.org/10.1021/bm034498j

Lavall, R.L., Assis, O.B., Campanafilho, S.P. 2007. Beta-chitin from the pens of Loligo sp.: extraction and characterization. Bioresource Technol. 98**,** 2465-2742.http://doi.org/10.1016/j.biortech.2006.09.002

Maghami, G.G., Roberts, G.A.F. 2010. Evaluation of the viscometric constants for chitosan. Macromol Chem Phys. 189**,** -.http://doi.org/10.1002/macp.1988.021890118

Mahlous, M., Tahtat, D., Benamer, S., Nacer Khodja, A. 2007. Gamma irradiation-aided chitin/chitosan extraction from prawn shells. Nuclear Instruments and Methods in Physics Research Section B: Beam Interactions with Materials and Atoms. 265**,** 414-417.https://doi.org/10.1016/j.nimb.2007.09.015

Mauricio-Sánchez, R.A., Salazar, R., Luna-Bárcenas, J.G., Mendoza-Galván, A. 2018. FTIR spectroscopy studies on the spontaneous neutralization of chitosan acetate films by moisture conditioning. Vib Spectrosc. 94**,** 1-6.https://doi.org/10.1016/j.vibspec.2017.10.005

Mazeau, K., Winter, W.T., Chanzy, H. 1994. Molecular and crystal structure of a high-temperature polymorph of chitosan from electron diffraction data. Macromolecules. 27**,** 7606-7612.http://doi.org/10.1021/ma00104a015

Menezes Maciel Bindes, M., Hespanhol Miranda Reis, M., Luiz Cardoso, V., Boffito, D.C. 2019. Ultrasound-assisted extraction of bioactive compounds from green tea leaves and clarification with natural coagulants (chitosan and Moringa oleífera seeds). Ultrason Sonochem. 51**,** 111-119.https://doi.org/10.1016/j.ultsonch.2018.10.014

Mohammed, M.H., Williams, P.A., Tverezovskaya, O. 2013. Extraction of chitin from prawn shells and conversion to low molecular mass chitosan. Food Hydrocolloid. 31**,** 166-171.http://doi.org/10.1016/j.foodhyd.2012.10.021

Osman, Z., Arof, A.K. 2003. FTIR studies of chitosan acetate based polymer electrolytes. Electrochim Acta. 48**,** 993-999.http://doi.org/10.1016/S0013-4686(02)00812-5

Pariser, E.R., Lombardi, D.P. 1989. Chitin sourcebook: a guide to the research literature. Wiley, New York, .

Paulino, A.T., Simionato, J.I., Garcia, J.C., Nozaki, J. 2006. Characterization of chitosan and chitin produced from silkworm crysalides. Carbohyd. Polym. 64**,** 98-103.https://doi.org/10.1016/j.carbpol.2005.10.032

Price, G.J. 2003. Recent developments in sonochemical polymerisation. Ultrason Sonochem. 10**,** 277-

283.https://doi.org/10.1016/S1350-4177(02)00156-6

Radhakumary, C., Antonty, M., Sreenivasan, K. 2011. Drug loaded thermoresponsive and cytocompatible chitosan based hydrogel as a potential wound dressing. Carbohyd. Polym. 83**,** 705-713.http://doi.org/10.1016/j.carbpol.2010.08.042

Ragetly, G.R., Slavik, G.J., Cunningham, B.T., Schaeffer, D.J., Griffon, D.J. 2010. Cartilage tissue engineering on fibrous chitosan scaffolds produced by a replica molding technique. J. Biomed. Mater. Res. A. 93A**,** 46-55.http://doi.org/10.1002/jbm.a.32514

Roberts, G.A.F. 1992. Chitin chemistry. Macmillan International Higher Education, Hong Kong. 368.https://doi.org/10.1007/978-1-349-11545-7

Safari, J., Javadian, L. 2015. Ultrasound assisted the green synthesis of 2-amino-4H-chromene derivatives catalyzed by Fe3O4-functionalized nanoparticles with chitosan as a novel and reusable magnetic catalyst. Ultrason Sonochem. 22**,** 341-348.https://doi.org/10.1016/j.ultsonch.2014.02.002

Sagheer, F.A.A., Al-Sughayer, M.A., Muslim, S., Elsabee, M.Z. 2009. Extraction and characterization of chitin and chitosan from marine sources in Arabian Gulf. Carbohyd. Polym. 77**,** 410-419.http://doi.org/10.1016/j.carbpol.2009.01.032

Sannan, T., Kurita, K., Iwakura, Y. 1975. Studies on chitin, 1. Solubility change by alkaline treatment and film casting. Die Makromolekulare Chemie. 176**,** 1191-1195.https://doi.org/10.1002/macp.1975.021760426

Sayari, N., Sila, A., Abdelmalek, B.E., Abdallah, R.B., Ellouz-Chaabouni, S., Bougatef, A., Balti, R. 2016. Chitin and chitosan from the Norway lobster by-products: Antimicrobial and anti-proliferative activities. Int J Biol Macromol. 87**,** 163-171.http://doi.org/10.1016/j.ijbiomac.2016.02.057

Shangan Lin, L.y., Zhaoxi Liang. 1998. Polysmer chemistry. Beijing: science Press.,

Simina, P.N., Jean-Michel, L., Catherine, L., Laurent, D., Alain, D. 2009. Mechanisms involved during the ultrasonically induced depolymerization of chitosan: characterization and control. Biomacromolecule. 10**,** 1203-1211.http://doi.org/10.1021/bm8014472

Tang, W., Wang, C., Chen, D. 2005. Kinetic studies on the pyrolysis of chitin and chitosan. Polym Degrad Stab. 87**,** 389-394.http://doi.org/10.1016/j.polymdegradstab.2004.08.006

Tokuyasu, K., Mitsutomi, M., Yamaguchi, I., Hayashi, K., Mori, Y. 2000. Recognition of chitooligosaccharides and their N-acetyl groups by putative subsites of chitin deacetylase from a deuteromycete, Colletotrichum lindemuthianum. Biochemistry. 39**,** 8837-8843.http://doi.og/10.1021/bi0005355

Wan, A.C., Tai, B.C. 2013. Chitin--a promising biomaterial for tissue engineering and stem cell technologies. Biotechnol Adv. 31**,** 1776-1785.http://doi.org/10.1016/j.biotechadv.2013.09.007

Wang, W., Bo, S.Q., Li, S.Q., Qin, W. 1991. Determination of the Mark-Houwink equation for chitosans with different degrees of deacetylation. Int J Biol Macromol. 13**,** 281-285.http://doi.org/10.1016/0141-8130(91)90027-r

Xu, D.-P., Zheng, J., Zhou, Y., Li, Y., Li, S., Li, H.-B. 2017. Ultrasound-assisted extraction of natural antioxidants from the flower of Limonium sinuatum: Optimization and comparison with conventional methods. Food Chem. 217**,** 552-559.https://doi.org/10.1016/j.foodchem.2016.09.013

Yao, Z.C., Jin, L.J., Ahmad, Z., Huang, J., Chang, M.W., Li, J.S. 2017. Ganoderma lucidum polysaccharide loaded sodium alginate micro-particles prepared via electrospraying in controlled deposition

environments. Int J Pharm. 524.http://doi.org/10.1016/j.ijpharm.2017.03.064

Tables

Table 1 Factors and levels of Taguchi orthogonal array design

Factor (i)	Level (j)		
	1	2	3
A: Time (min)	10	20	30
B: NaOH (%, g/mL)	10	20	30
C: Solid-liquid ratio	1:15	1:20	1:25
D: Power (W)	80	120	160

Table 2 The CrI and 2θ of chitosan obtained from various irradiation time

Sample (min)	Results	
	CrI (%)	2θ (°)
5	68.27	9.0,19.68,20.90,22.0,22.78,23.58
10	70.28	9.3,19.68,20.90, 27.5, 31.9,
20	67.11	9.06,19.68,20.94,23.64,
30	71.35	9.06,19.68,20.90,22.88,23.6,32.13

Table 3 The weight loss of resultant chitosan with temperature rising

Temperature interval (±2℃)	Weight loss ($\frac{\Delta m}{m_0}$×100%) of chitosan obtained from irradiation time (min)			
	5	10	20	30
31-128	4.98	7.43	10.25	7.45
129-369	24.44	26.20	26.05	24.95
370-477	42.82	46.77	37.39	48.12
478-700	1.73	1.37	1.36	1.18
Residual weight (%)	26.03	18.23	24.95	18.3

Δm: the lost weight at every temperature interval, m_0: the initial weight of each chitosan sample.

Table 4 Results of orthogonal experiment

Run #	Time (min)	Power (W)	NaOH (%, g: ml)	Solid-liquid ratio (g: mL)	DD (%)	$[\eta]$ (cP)	$\overline{Mv}$ (g/mol)
1	10	80	10	1:15	81.08 c	13.94	6126.88
2	10	120	20	1:20	83.02 abc	15.33	6696.22
3	10	160	30	1:25	83.99 a	18.65	8033.21
4	20	80	30	1:20	81.55 bc	15.86	6909.56
5	20	120	20	1:25	81.95 bc	14.97	6546.59
6	20	160	10	1:15	81.43 bc	17.34	7506.48
7	30	80	20	1:25	82.98 abc	24.23	10248.21
8	30	120	30	1:15	83.33 ab	13.81	6073.49
9	30	160	10	1:20	80.75 d	9.56	4313.01
ANOVA analysis							
SS	1.7314	1.3429	6.0349	2.5240			
Df	2	2	2	2			
F	20.558	7.910	110.733	25.828			
P-value	0.000*	0.003*	0.000*	0.000*			
Range analysis							
K_{i1}	82.6967	81.87	81.086	81.9467			
K_{i2}	81.6433	82.766	82.65	81.7733			
K_{i3}	82.3533	82.056	82.956	82.9733			
R_j	1.0533	0.8967	1.87	1.0267			

K_{ij}: the average response of each factor at various levels, i: factor, j: level;

R_j: K_{Lmax}- K_{Lmin} for each factor;

SS: sum of sequares;

Df: degree of freedom.

[a] Means within a column for DD value followed by the same letter was not significantly different at $p < 0.05$ (Tukey HSD test).

Figure legends

Figure 1 A schematic diagram of the USAD setup (a) and effect of irradiation time on temperature of the transducer and the GLS suspension (b).

Figure 2 Effect of irradiation parameters on DD, [η], $\overline{Mv}$, and yield: a: time; b: power; c: concentration of NaOH; d: solid-liquid ratio (w/v); e: duty cycle; f: effects of irradiation time on yield of chitosan.

Figure 3 Effects of USAD with various time on surface morphology of chitosan: a, GLSP; b- e, USAD with 5, 10, 20 and 30 min respectively, which combined with the other parameters were: NaOH concentration (10%, g: mL), power (80 W), solid-liquid ratio (1:15, g: mL), duty cycle (30:1).

Figure 4 FT-IR results (a) and XRD results (b) of chitosan.

Figure 5 TG results (a) and DTG results (b) of resultant chitosan.

Figures

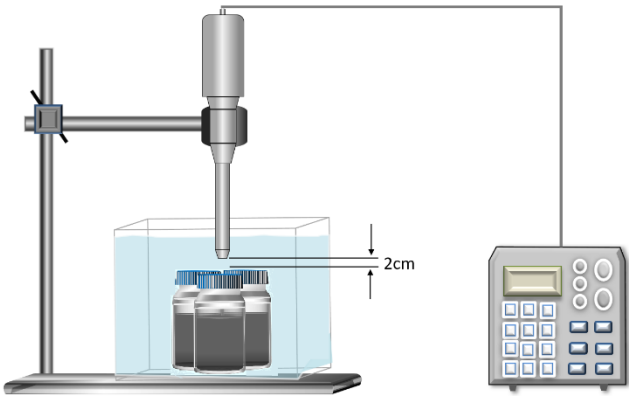

Figure 1

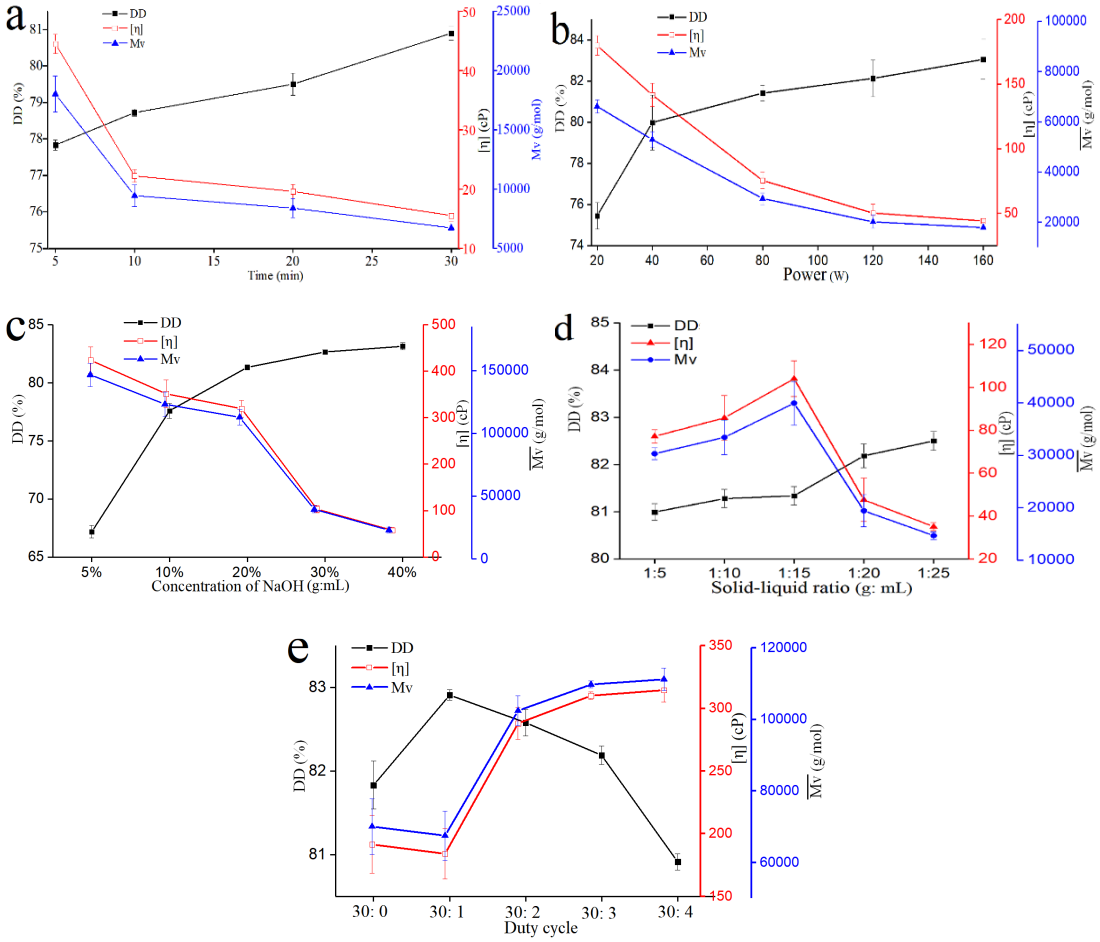

Figure 2

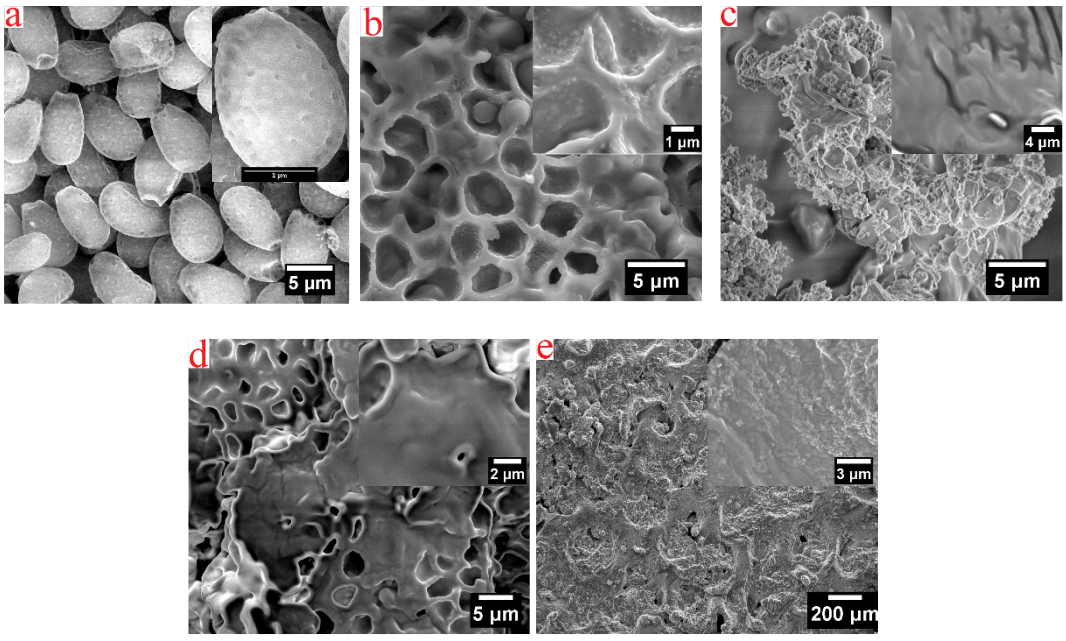

Figure 3

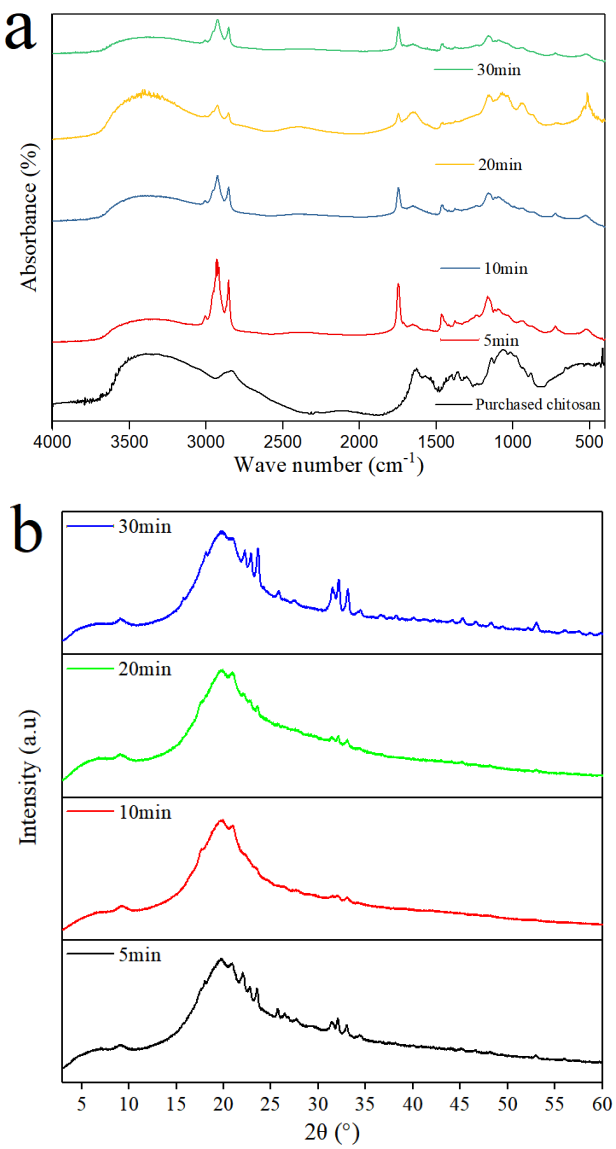
a
30min
20min
10min
5min
Purchased chitosan
Absorbance (%)
4000
3500
3000
2500
2000
1500
1000
500
Wave number (cm-1)
b
30min
20min
10min
5min
Intensity (a.u)
5
10
15
20
25
30
35
40
45
50
55
60
2θ (°)

Figure 4

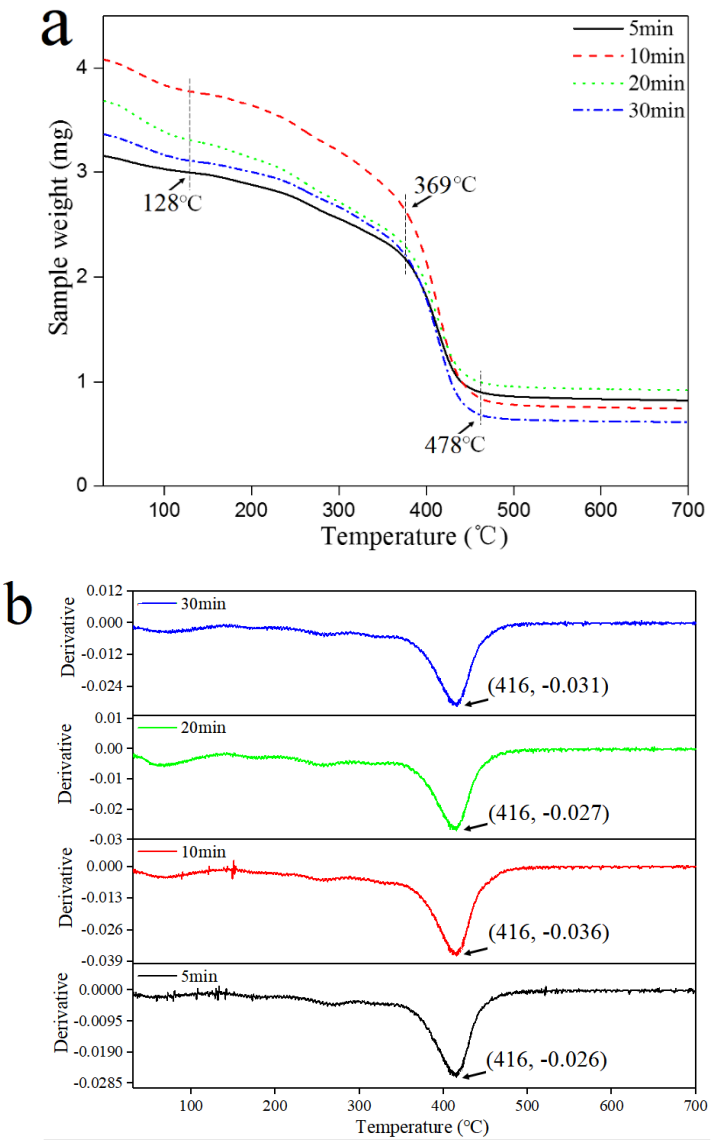
a
5min
10min
20min
30min
Sample weight (mg)
128℃
369℃
478℃
Temperature (℃)
b
30min
Derivative
(416, -0.031)
20min
(416, -0.027)
10min
(416, -0.036)
5min
(416, -0.026)
Temperature (℃)

Figure 5